Available online at www.sciencedirect.com
ScienceDirect
Trans. Nonferrous Met. Soc. China 31(2021) 3150−3161
Transactions of Nonferrous Metals Society of China
www.tnmsc.cn

Complexation extraction of scheelite and transformation behaviour of tungsten-containing phase using H_2SO_4 solution with $H_2C_2O_4$ as complexing agent

Qing-sheng LIU[1], Tao TU[1,2], Hao GUO[3], Hua-jin CHENG[1], Xue-zhong WANG[1]

1. Faculty of Materials Metallurgy and Chemistry,
Jiangxi University of Science and Technology, Ganzhou 341000, China;
2. Mechanical and Electrical Engineering Department,
Gannan University of Science and Technology, Ganzhou 341000, China;
3. School of Materials Science and Engineering, Jiangsu University, Zhenjiang 212013, China

Received 20 September 2020; accepted 31 July 2021

Abstract: The extraction of tungsten from scheelite was carried out using a sulfuric acid solution with oxalic acid as the chelating agent. Tungsten was obtained in the form of highly soluble hydrogen aqua oxalato tungstate ($H_2[WO_3(C_2O_4)\cdot H_2O]$) during the leaching process, while calcium remained in the residue as calcium sulfate dihydrate ($CaSO_4\cdot 2H_2O$). About 99.2% of the tungsten was leached at 70 °C, 1.5 mol/L sulfuric acid, 1 mol/L oxalic acid, a liquid/solid ratio of 25:1 (mL/g), an oxalic acid to sulfuric acid molar ratio of 1:1, a stirring speed of 300 r/min and a leaching time of 2 h. $H_2[WO_3(C_2O_4)\cdot H_2O]$ was thermally decomposed into tungstic acid (H_2WO_4), and tungsten trioxide (WO_3) was directly produced by calcining H_2WO_4 at 700 °C for 2 h. The surface chemical reaction was determined to be the controlling step during tungsten leaching, and the apparent activation energy was calculated to be 51.43 kJ/mol.
Key words: scheelite; kinetics; chemical reaction; oxalic acid; sulfuric acid

1 Introduction

Tungsten is widely used in transportation, mechanical engineering, and manufacturing applications owing to its outstanding physical and mechanical properties and high chemical stability, especially at high temperatures [1,2]. Tungsten usually exists in nature in hexavalent form. The most important tungsten ore minerals are scheelite ($CaWO_4$) and wolframite ($(Fe,Mn)WO_4$), while scheelite alone accounts for two-third of the global tungsten ore reserves [3]. As high-grade wolframite ore is being rapidly consumed, the extraction of tungsten from low-grade scheelite ore resources is becoming increasingly common to maintain the sustainable supply of this important metal.

The most common process for extracting tungsten from scheelite involves the alkali leaching in an autoclave to decompose the mineral [4−7]. In Western countries, sodium carbonate is often used as the alkali in the autoclave method, whereas sodium hydroxide is mainly used in China. Because the leaching reaction has a low equilibrium constant, scheelite cannot be effectively processed at room temperature and atmospheric pressure. To achieve a high tungsten leaching rate, high temperatures, pressures, and reagent concentrations are required, along with the specialized hydrometallurgy equipment that can withstand these extreme conditions. In addition, this process inevitably discharges large amount of alkali

Corresponding author: Qing-sheng LIU, Tel: +86-15970132969, E-mail: lqs_01259@126.com
DOI: 10.1016/S1003-6326(21)65724-2

leachate after ion exchange, causing environmental pollution [8].

Compared with the high-pressure alkali decomposition of scheelite, the decomposition of scheelite concentrate with hydrochloric acid has a high equilibrium constant and can be performed at atmospheric pressure [9]. However, hydrochloric acid decomposition of scheelite can produce a solid layer of tungstic acid (hydrated form of WO_3) on the surface of unreacted particles [10], which increases in thickness as the leaching time increases. Eventually, the reaction rate decreases as the tungstic acid layer limits the diffusion of hydrochloric acid to the reaction interface with the scheelite [11]. To reduce the reaction time and increase the leaching efficiency, alternative methods have been proposed. For example, LI [12] proposed that scheelite could be leached using hydrochloric acid equivalent to nearly 1.5 times the stoichiometric proportion. He used tungstic acid to prepare ammonium paratungstate (an ammonium secondary tungstate), and then treated the leachate containing calcium chloride prior to ion exchange. Although such methods can minimize the negative effects of tungstic acid on the process, they also have some disadvantages. For example, the use of extremely small scheelite particles can increase the production cost, while the highly concentrated hydrochloric acid makes the leachate highly volatile and corrosive, which significantly increases the demands associated with the equipment and safety protocols of the entire leaching operation.

Sulfuric acid has been proposed as an alternative reagent for decomposing scheelite concentrate to avoid the use of hydrochloric acid. As sulfuric acid is relatively inexpensive and non-volatile, it can be used to reduce the material cost and increase the safety of the operating environment. However, similar to the use of HCl, tungstic acid can hinder the reaction, and cannot be easily separated from the calcium sulfate precipitate. LI and ZHAO [13] used a sulfuric/phosphoric acid mixture as a leaching agent to decompose scheelite. The tungsten in scheelite ore was completely leached in a highly soluble form of phosphotungstic acid ($H_3PW_{12}O_{40}$), whereas the calcium remained in the residue in the form of calcium sulfate ($CaSO_4{\cdot}nH_2O$). Although phosphoric acid can prevent tungstic acid from hindering scheelite decomposition, this chelating agent inevitably produces non-volatile phosphorus impurities during leaching, which can act as environmental pollutants. Therefore, new methods for efficiently extracting tungsten from scheelite need to be developed that meet the economic and environmental targets of the industry. For example, KALPAKLI et al [14] showed that the dissolution of calcium tungstate in oxalic acid solution results in the formation of water-soluble hydrogen aqua oxalato tungstate ($H_2[WO_3(C_2O_4){\cdot}H_2O]$) and insoluble calcium oxalate monohydrate ($CaC_2O_4{\cdot}H_2O$). Compared with phosphoric acid, oxalic acid has better environmental adaptability as an organic acid.

To efficiently leach scheelite and reduce environmental pollution, we used oxalic acid as a chelating agent to leach scheelite in a sulfuric acid solution. We also analyzed the effects of stirring speed, temperature, oxalic-to-sulfuric acid concentration ratio ($c(H_2C_2O_4)/c(H_2SO_4)$), leaching time, and liquid-to-solid ratio on the leaching rate of tungsten. The leaching residue produced under different processing conditions was characterized using X-ray diffraction (XRD). In addition, we investigated the dynamics of the leaching process and the apparent activation energy. After leaching scheelite, the leaching solution was heated to form tungstic acid, and then calcined to produce high-purity tungsten trioxide, which is the most common precursor of tungsten metal.

2 Experimental

2.1 Materials

The scheelite concentrate was provided by a company in Jiangxi Province, China. The chemical composition of the concentrate is listed in Table 1, where the main components were W (44.04%), Ca (12.49%), and Si (2.56%). The XRD pattern of the scheelite concentrate (Fig. 1) shows that the main phases are calcium tungstate, calcium carbonate, and silicon dioxide (silica). Scanning electron microscopy-energy dispersive X-ray spectroscopy (SEM-EDS) analysis was performed on the scheelite concentrate, and the results are shown in Fig. 2. There is a strong overlap between W and Si, indicating that these elements exist in the same compounds. Similarly, S, Fe, and Cu have similar distributions. In addition, Ca overlaps weakly with W or Si. All the elements overlap with O, indicating that these elements exist as oxides. The other

reagents and solutions used in this experiment are of analytical grade.

Table 1 Chemical composition of scheelite concentrate (wt. %)

Si	P	Cl	S	Ca	Fe	Cu	W
2.56	0.38	0.15	0.92	12.49	1.99	1.04	44.04

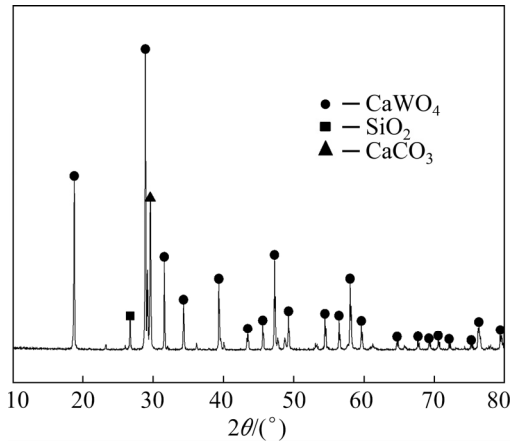

Fig. 1 XRD pattern of scheelite concentrate

2.2 Methods

2.2.1 Leaching experiments

The leaching experiments were conducted by putting the solution in a 250 mL round-bottom flask and then heating the solution in a water bath. A condensing tube was used to prevent solution loss caused by evaporation. The leaching conditions were varied over suitable ranges to separately investigate the effect of stirring speed (200−400 r/min), liquid/solid ratio (10:1−30:1 mL/g), molar ratio of oxalic to sulfuric acid $n(H_2C_2O_4)/n(H_2SO_4)$ (0.14:1−7:1), sulfuric acid concentration (0.5−2.5 mol/L), oxalic acid concentration (0.3−1.6 mol/L), leaching temperature (40−80 °C), and leaching time (0.5−2.5 h). After leaching, the solution was filtered to separate the solids. The tungsten content in the leaching solution was determined using inductively coupled plasma-optical emission spectrometry (ICP-OES). The leaching rate of tungsten (E) was calculated using the following equation:

$$E=\frac{CV}{mw}\times 100\% \quad (1)$$

where C is the concentration of tungsten in the leaching solution (g/L); V is the volume of the leaching solution (L); m is the mass of the scheelite (g); w is the tungsten content of the scheelite (wt.%).

2.2.2 Decomposition of leaching solution

The leaching solution obtained after leaching scheelite in the sulfuric and oxalic acid mixture was heated to 85 °C for 3 h, in which tungstic acid formed as a precipitate. After filtering, the tungstic acid was calcined for 2 h at 700 °C to form tungsten trioxide. The micromorphology and phase composition of the calcined products were investigated using SEM and XRD.

2.3 Characterization

The elemental composition of the materials was determined using X-ray fluorescence spectroscopy (ARL ADVANT'X Intellipower 4200, ThermoFisher, USA). The crystalline mineral phases of the scheelite and leaching residue were determined using XRD (SMART APEXII, Bruker AXS GmbH, Germany). The microstructures of the scheelite and leaching residue were characterized by field emission SEM (MLA 650F, FEI Company,

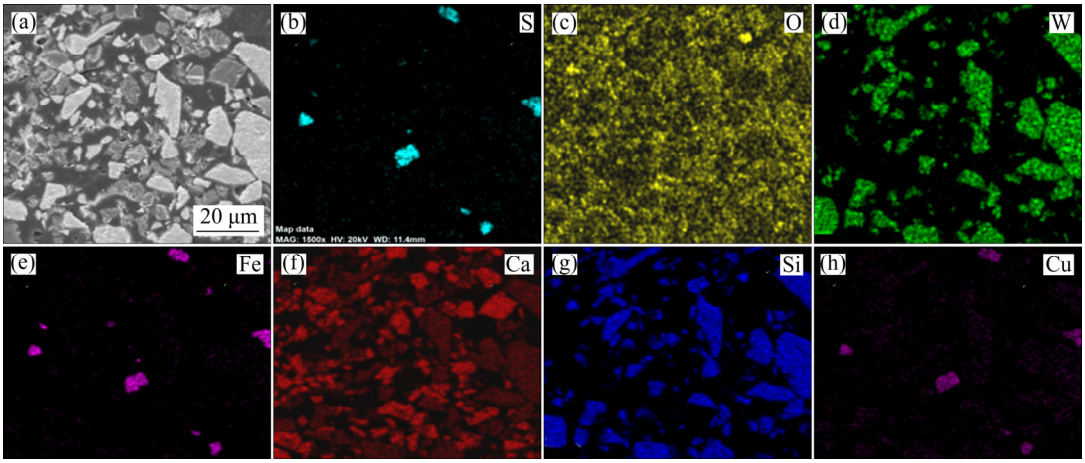

Fig. 2 SEM image (a) and EDS elemental distributions (b−h) of scheelite concentrate

USA). The elemental distributions of the scheelite and leaching residue were determined by EDS mapping (Neptune TEXS HP, Edax, Japan). The tungsten content of the leaching solution was determined by ICP-OES (iCAP 6300, Thermo Fisher Scientific, USA).

3 Results and discussion

3.1 Leaching of scheelite

3.1.1 Stirring speed

The effect of stirring speed (200−400 r/min) on the leaching rate of tungsten was analyzed, while the other conditions were kept constant: temperature, 70 °C; sulfuric acid concentration, 1.5 mol/L; oxalic acid concentration, 1 mol/L; liquid/solid ratio, 25:1 (mL/g); $n(H_2C_2O_4)/n(H_2SO_4)$ ratio, 1:1; leaching time, 2 h. The leaching rate of tungsten and the XRD patterns of the corresponding leaching residue at different stirring speeds are shown in Figs. 3(a) and (b), respectively. As shown in Fig. 3(a), when the stirring speed increased from 200 to 400 r/min, the tungsten leaching rate gradually increased from 98.3% to 99%. The tungsten leaching rate is only slightly dependent on the stirring speed, implying that the leaching of scheelite is limited by the chemical reaction step. The main phase of the leaching residue for all stirring speeds was calcium sulfate dihydrate ($CaSO_4·2H_2O$) (Fig. 3(b)). To obtain an optimal leaching efficiency of tungsten from scheelite, 300 r/min was used for all further experiments.

3.1.2 Liquid/solid ratio

The effect of liquid/solid ratio (10:1−30:1 (mL/g)) on the leaching rate of tungsten is shown in Fig. 4(a), where all other parameters were kept constant, as described above. The tungsten leaching rate increased with increasing liquid/solid ratio. Specifically, when the liquid/solid ratio increased from 10:1 to 25:1 (mL/g), the tungsten leaching rate increased from 94.5% to 99%. However, when the liquid/solid ratio was further increased to

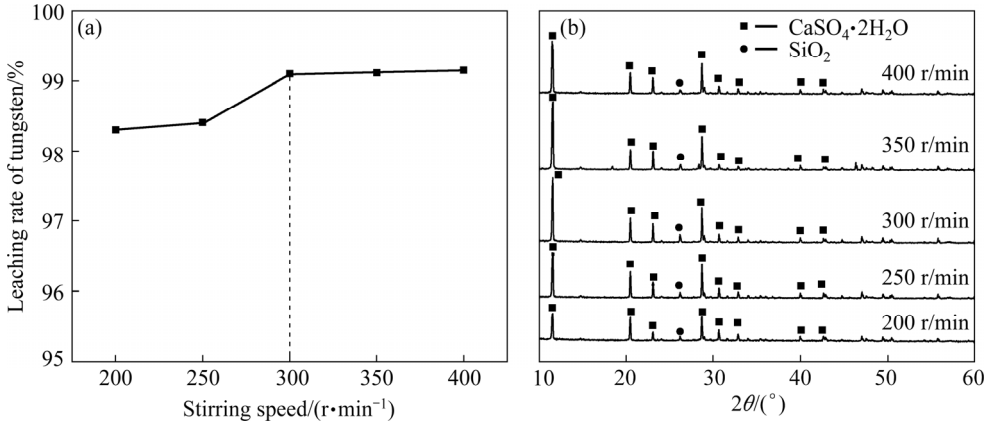

Fig. 3 Effect of stirring speed on leaching rate of tungsten (a) and XRD patterns of leaching residue (b) (70 °C; 1.5 mol/L H_2SO_4; 1 mol/L $H_2C_2O_4$; liquid/solid ratio 20:1; $n(H_2C_2O_4)/n(H_2SO_4)$ ratio 1:1; 2 h)

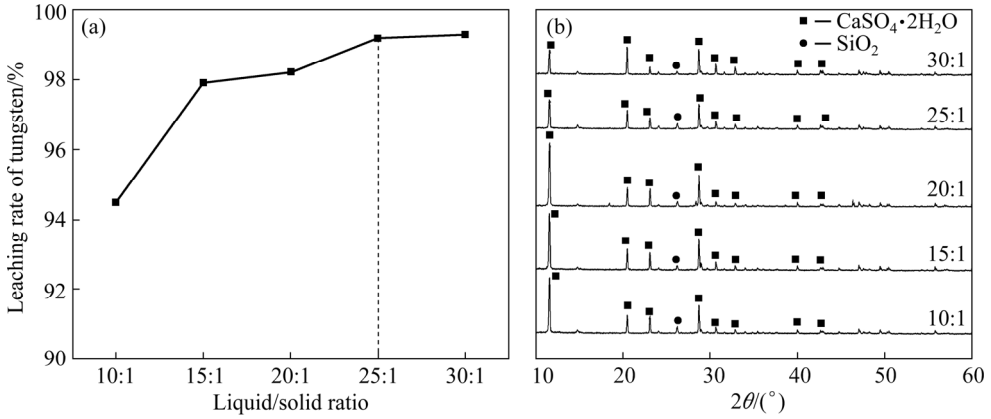

Fig. 4 Effect of liquid/solid ratio on leaching rate of tungsten (a) and XRD patterns of leaching residue (b) (70 °C; 1.5 mol/L H_2SO_4; 1 mol/L $H_2C_2O_4$; 300 r/min; $n(H_2C_2O_4)/n(H_2SO_4)$ ratio 1:1; 2 h)

30:1 (mL/g), the tungsten leaching rate remained unchanged. The XRD patterns of the corresponding leaching residue with different liquid/solid ratios are shown in Fig. 4(b). The intensity of the main diffraction peaks (attributed to calcium sulfate dihydrate) increased with increasing liquid/solid ratio. Changing the liquid/solid ratio did not have a significant effect on any of the crystalline phases in the leaching residue.

3.1.3 Oxalic to sulfuric acid molar ratio

As the total acidity of the solution was kept constant throughout the experiments, the amount of H^+ in the solution remained constant. The effects of $n(H_2C_2O_4)/n(H_2SO_4)$ ratios on the tungsten leaching rate and XRD patterns of the residue are shown in Figs. 5(a) and (b), respectively.

As shown in Fig. 5(a), there was a rapid increase in the leaching rate of tungsten, from 22.9% to 99.2% as the $n(H_2C_2O_4)/n(H_2SO_4)$ ratio increased from 0.14:1 to 1:1. Initially, low tungsten leaching rates of 22.9% and 63.8% were measured at $n(H_2C_2O_4)/n(H_2SO_4)$ ratios of 0.14:1 and 0.45:1, respectively. These low leaching rates are ascribed to the low concentration of oxalic acid in the mixture and the dominant role of sulfuric acid. According to Reaction (2), when sulfuric acid is dominant, tungstic acid covers the unreacted mineral grains and significantly hinders the leaching of the grains, resulting in a low tungsten leaching rate. When the $n(H_2C_2O_4)/n(H_2SO_4)$ ratio increased to 1:1, the tungsten leaching rate significantly increased to 95.6%. As the $n(H_2C_2O_4)/n(H_2SO_4)$ ratio increased further, the tungsten leaching rate remained unchanged, but the diffraction pattern of calcium oxalate monohydrate ($CaC_2O_4·H_2O$) appeared. According to Reaction (3), when the oxalic acid concentration is dominant in the mixed solution, water-soluble hydrogen aqua oxalato tungstate ($H_2[WO_3(C_2O_4)·H_2O]$) is formed instead of tungstic acid monohydrate ($H_2WO_4·H_2O$). In Fig. 5(b), the diffraction peak of $H_2WO_4·H_2O$ disappeared with increasing $n(H_2C_2O_4)/n(H_2SO_4)$ ratio. Therefore, the $n(H_2C_2O_4)/n(H_2SO_4)$ ratio of 1:1 was considered to be optimal and was used for further experiments on the decomposition of scheelite.

$$CaWO_{4(s)}+H_2SO_{4(aq)}+3H_2O= CaSO_4·2H_2O_{(s)}+H_2WO_4·H_2O_{(s)} \quad (2)$$

$$CaWO_{4(s)}+2H_2C_2O_{4(aq)}+H_2O= CaC_2O_4·H_2O_{(s)}+H_2[WO_3(C_2O_4·H_2O]_{(aq)} \quad (3)$$

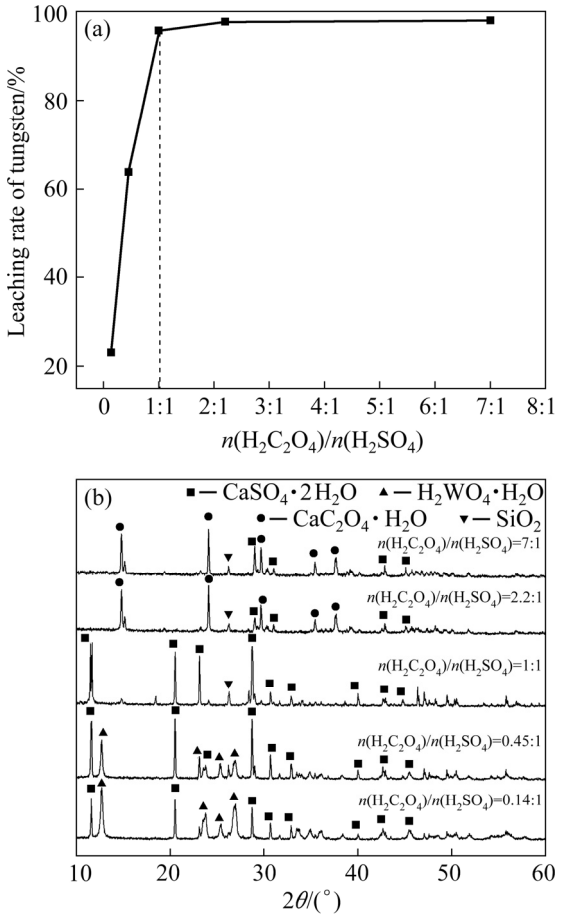

Fig. 5 Effect of $n(H_2C_2O_4)/n(H_2SO_4)$ ratio on leaching rate of tungsten (a) and XRD patterns of leaching residue (b) (70 °C; 1.5 mol/L H_2SO_4; 1 mol/L $H_2C_2O_4$; 300 r/min; liquid/solid ratio 25:1; 2 h)

3.1.4 Sulfuric acid concentration

Figure 6(a) shows the effect of sulfuric acid concentration (0.5−2.5 mol/L) on the tungsten leaching rate, while all other conditions were fixed, as described above. The XRD patterns of the corresponding leaching residues are shown in Fig. 6(b). When the sulfuric acid concentration increased from 0.5 to 1.5 mol/L, the tungsten leaching rate increased from 93.8% to 99.2%. As shown in Fig. 6(b), calcium oxalate monohydrate was the main crystalline phase in the leaching residue. However, as the sulfuric acid concentration increased further to 2.5 mol/L, the tungsten leaching rate rapidly decreased to 74.7%. In addition, as the sulfuric acid concentration increased, only a small amount of oxalic acid was present in the solution, and some of the produced tungstic acid was not chelated by the oxalic acid. Therefore, some tungstic acid remained in the leaching residue, which decreased the overall

leaching rate. With increasing sulfuric acid concentration, the diffraction peak of calcium oxalate monohydrate in the leaching residue disappeared, whereas that of calcium sulfate dihydrate started to appear.

3.1.5 Oxalic acid concentration

The effect of oxalic acid concentration (0.3−1.6 mol/L) on the leaching rate of tungsten is shown in Fig. 7(a), and the corresponding XRD patterns of the leaching residue are shown in Fig. 7(b). The lowest oxalic acid concentration of 0.3 mol/L achieved a tungsten leaching rate of only 52.4%, because there was insufficient oxalic acid in the solution to fully chelate the tungstic acid and form the precipitate. Figure 7(b) shows calcium sulfate dihydrate and tungstic acid monohydrate as the main crystalline phases in the leaching residue. When the oxalic acid concentration increased from 0.3 to 1 mol/L, the tungsten leaching rate also increased from 52.4% to 99.2%, respectively, whereas the diffraction peak of tungstic acid monohydrate was steadily weakened before eventually disappearing. With increasing oxalic acid concentration, tungstic acid and oxalic acid chelate formed hydrogen aqua oxalato tungstate, where the main phase of leaching residue was calcium sulfate dihydrate. When the oxalic acid concentration increased to 1.6 mol/L, the tungsten leaching rate decreased to 95.6%, and calcium sulfate dihydrate and calcium oxalate monohydrate were the main phases of the leaching residue. Therefore, the optimal oxalic acid concentration was 1 mol/L.

3.1.6 Leaching temperature

The effect of temperature on the leaching rate of tungsten was investigated by increasing the temperature from 40 to 80 °C. Figure 8(a) shows that the tungsten leaching rate is extremely sensitive to temperature changes and increases with increasing temperature. The tungsten leaching rate was only 74.4% at 40 °C because of the low

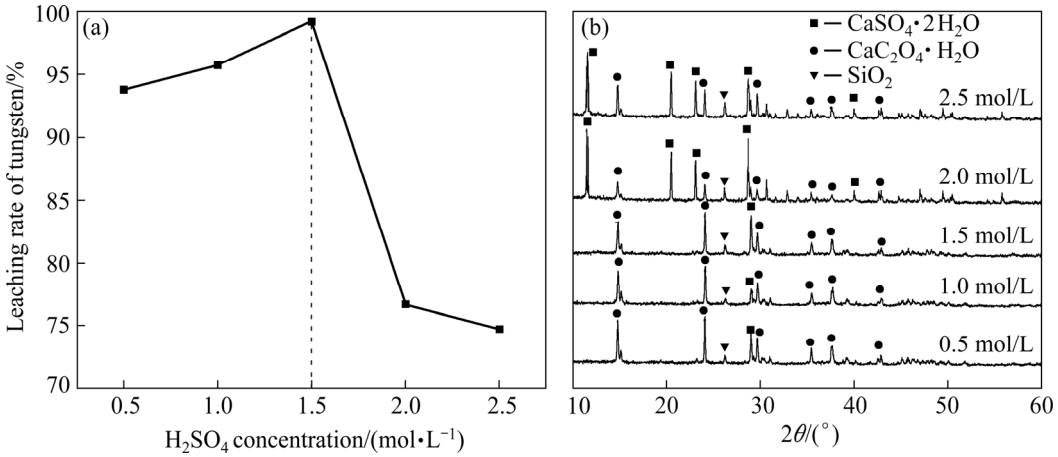

Fig. 6 Effect of H_2SO_4 concentration on leaching rate of tungsten (a) and XRD patterns of leaching residue (b) (70 °C; 1 mol/L $H_2C_2O_4$; 300 r/min; liquid/solid ratio 25:1; $n(H_2C_2O_4)/n(H_2SO_4)$ ratio 1:1; 2 h)

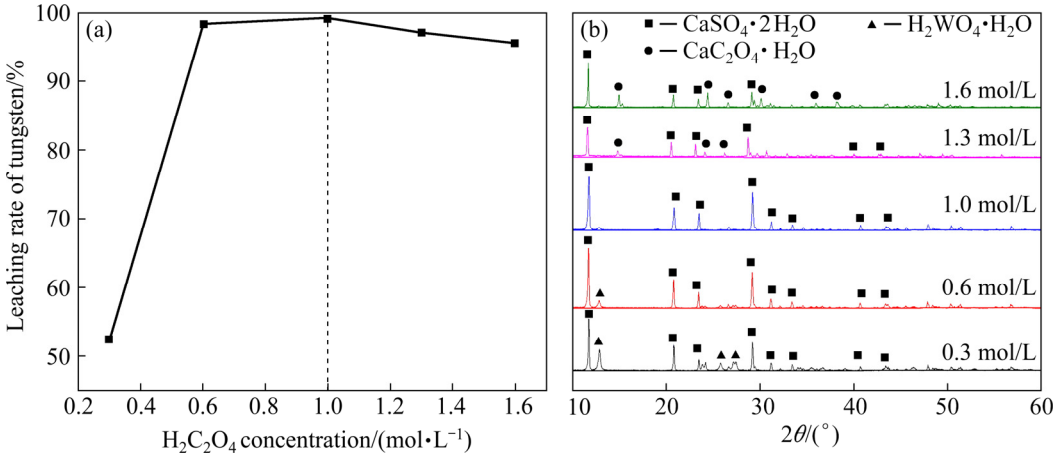

Fig. 7 Effect of $H_2C_2O_4$ concentration on leaching rate of tungsten (a) and XRD patterns of leaching residue (b) (70 °C; 1.5 mol/L H_2SO_4; 300 r/min; liquid/solid ratio 25:1; $n(H_2C_2O_4)/n(H_2SO_4)$ ratio 1:1; 2 h)

reaction rate at low temperature, where calcium sulfate dihydrate and calcium oxalate monohydrate were the main phases in the leaching residue (Fig. 8(b)). When the temperature increased to 50 °C, the leaching rate of tungsten increased to 93.7%. The main phase in the leaching residue was calcium sulfate dihydrate, and the diffraction peak of calcium oxalate monohydrate was not observed. Increasing the temperature further resulted in a maximum tungsten leaching rate of 99.2% being achieved at 70 °C, accompanied by a strong diffraction peak of calcium sulfate dihydrate. Therefore, 70 °C was considered as the optimal temperature.

3.1.7 Leaching time

The effect of leaching time on the leaching rate of tungsten was investigated by increasing the leaching time from 0.5 to 2.5 h (Fig. 9(a)). The XRD patterns of the corresponding leaching residue at different time are shown in Fig. 9(b). As shown in Fig. 9(a), for a tungsten leaching time of 0.5 h, a tungsten leaching rate of 90.4% was achieved. This extremely short reaction time did not allow the reaction to reach completion, and some of the scheelite remained in the slag. Figure 9(b) shows calcium tungstate and calcium sulfate dihydrate as the main phases in the leaching residue reacted for 0.5 h. The tungsten leaching rate reached the maximum of 99.2% after 2 h of leaching. The diffraction peak of calcium tungstate was weakened over time, whereas that of calcium sulfate dihydrate gradually increased. Thus, a leaching time of 2 h was appropriate.

3.2 Scheelite leaching mechanism

Based on the experimental results presented above, the optimal leaching conditions for extracting tungsten from scheelite were identified as follows: stirring speed, 300 r/min; sulfuric acid concentration, 1.5 mol/L; oxalic acid concentration,

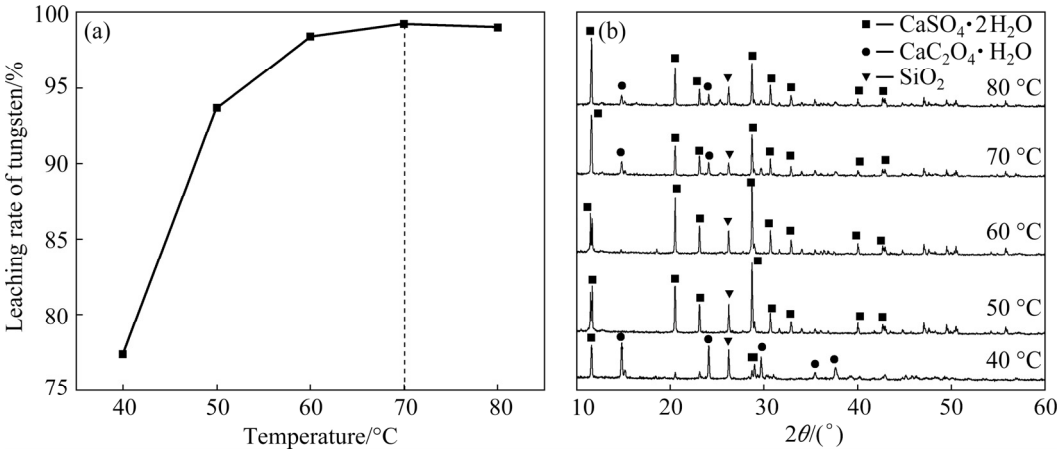

Fig. 8 Effect of temperature on leaching rate of tungsten (a) and XRD patterns of leaching residue (b) (1 mol/L $H_2C_2O_4$; 1.5 mol/L H_2SO_4; 300 r/min; liquid/solid ratio 25:1; $n(H_2C_2O_4)/n(H_2SO_4)$ ratio 1:1; 2 h)

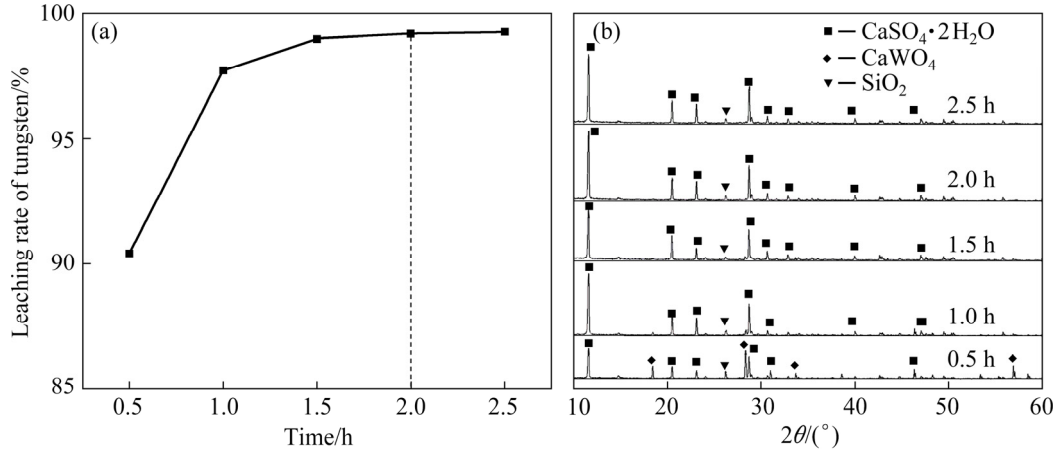

Fig. 9 Effect of time on leaching rate of tungsten (a) and XRD patterns of leaching residue (b) (70 °C; 1 mol/L $H_2C_2O_4$; 1.5 mol/L H_2SO_4; 300 r/min; liquid/solid ratio 25:1; $n(H_2C_2O_4)/n(H_2SO_4)$ ratio 1:1)

1 mol/L; temperature, 70 °C; liquid/solid ratio, 25:1 (mL/g); $n(H_2C_2O_4)/n(H_2SO_4)$ ratio, 1:1; leaching time, 2 h. The XRD patterns and SEM-EDS images of the leaching residue under optimal conditions are shown in Figs. 10 and 11, respectively. Figure 10 shows that the main phases of the leaching residue were calcium sulfate dihydrate and silicon dioxide. The distributions of S and Ca, Si and O, and Fe and Cu were similar, as shown in Fig. 11. Compared with the EDS results of the original scheelite shown in Fig. 2, the tungsten content of the raw material was much lower, indicating that tungsten was leached effectively.

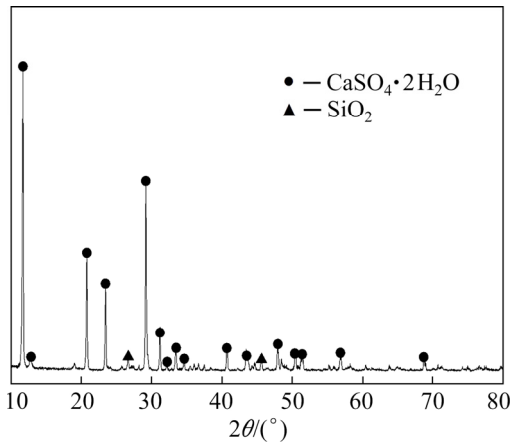

Fig. 10 XRD pattern of leaching residue under optimal conditions

During the leaching of scheelite, tungsten can react with both sulfuric and oxalic acids. Scheelite initially reacts with sulfuric acid to produce tungstic acid and calcium sulfate. However, separating tungstic acid from the calcium sulfate solids and the unreacted ore particles introduces a challenge that may severely impede the tungsten leaching process and limit the leaching efficiency. Upon introducing oxalic acid as a chelating agent, insoluble tungstic acid is converted into highly soluble hydrogen aqua oxalato tungstate, which can increase the tungsten leaching rate compared to the use of sulfuric acid alone. Scheelite reacts with a sulfuric and oxalic acid mixture according to Eq. (4), which shows that hydrogen aqua oxalato tungstate increases the overall water solubility of tungsten-containing compounds and increases the tungsten leaching rate.

$$CaWO_{4(s)}+H_2C_2O_{4(aq)}+H_2SO_{4(aq)}+2H_2O= CaSO_4·2H_2O_{(s)}+H_2[WO_3(C_2O_4)·H_2O]_{(aq)} \quad (4)$$

3.3 Kinetics of scheelite leaching

In the leaching of tungsten from scheelite concentrate using sulfuric and oxalic acids, the reaction kinetics is controlled by: the external diffusion of the leaching agent through the boundary layer; internal diffusion through the solid layer; chemical reactions on the particle surface; and their combined control [15]. In this study, the shrinking core model (SCM) was used to describe the leaching behaviour controlled by the reaction step with the slowest kinetics [16−18]. The rate equations of the SCM model can be simplified to describe the rate-limiting steps of the chemical reactions, internal diffusion, and the combination of these steps, as shown in Eqs. (5), (6), and (7), respectively.

$$1-(1-x)^{1/3}=k_1t \quad (5)$$

$$1-2/3x-(1-x)^{2/3}=k_2t \quad (6)$$

$$1-(1-x)^{1/3}-1/3\ln(1-x)=k_3t \quad (7)$$

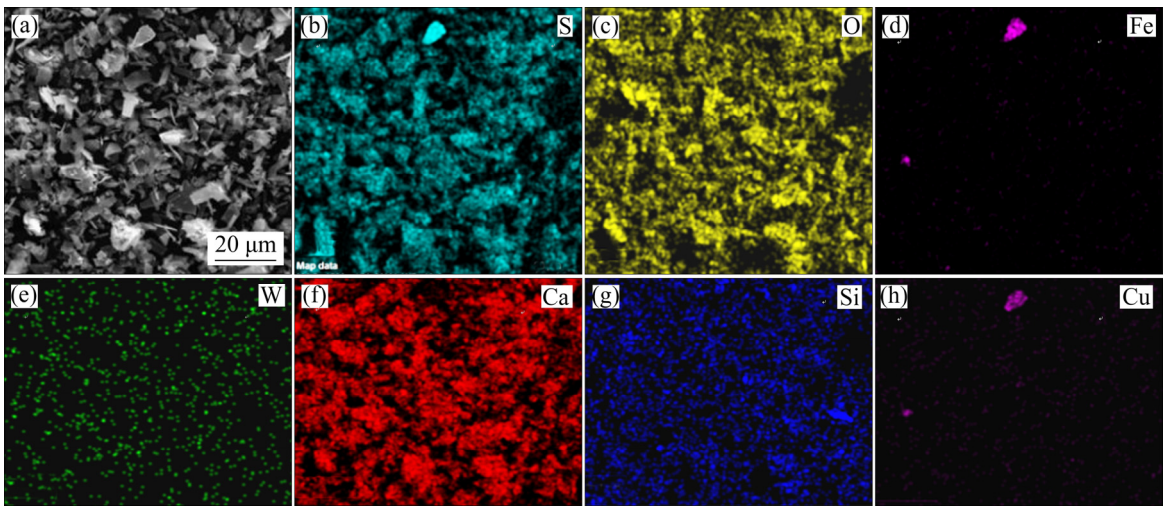

Fig. 11 SEM image (a) and EDS elemental distributions (b−h) of leaching residue under optimal conditions

where x is leaching rate of tungsten (%), t is leaching time (min), and k_1, k_2 and k_3 are rate constant (min^{-1}), respectively.

The time-dependent tungsten leaching rate curves at different temperatures (Fig. 12) clearly show that the leaching rate increases with increasing temperature. Figure 13 shows the relationships between different kinetic model functions and time, while the fitted straight lines are the corresponding curves using the three kinetic models at 60 °C. The experimental data show the highest correlation coefficient (R^2=0.992) when they are fitted with Eq. (5), indicating that the leaching process of tungsten from scheelite is controlled by the chemical reactions.

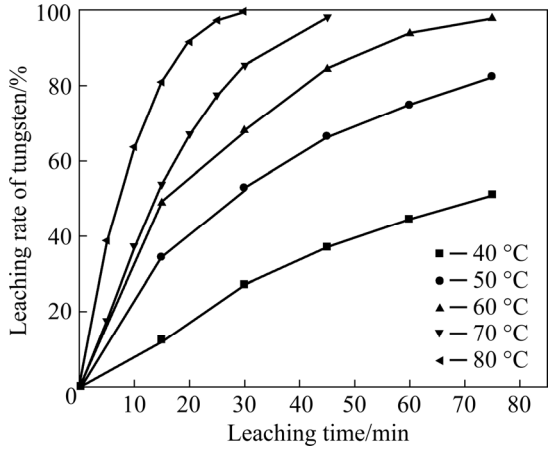

Fig. 12 Effect of time on leaching rate of tungsten at different temperatures

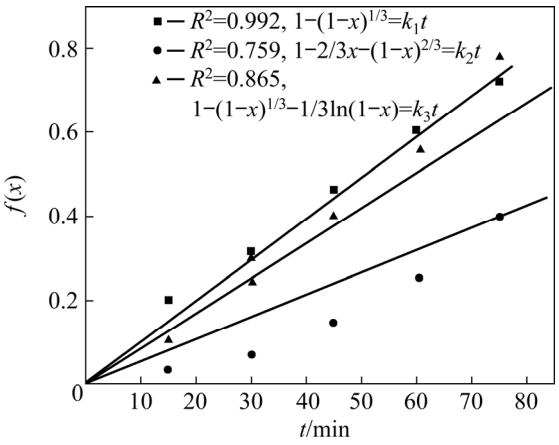

Fig. 13 Fitted lines of three kinetic models at 60 °C

The reaction constants at different temperatures follow the Arrhenius equation (Eq. (8)) [19,20]:

$$k=A\exp[-E_a/(RT)] \quad (8)$$

where A is pre-exponential factor, k is the reaction rate constant (min^{-1}), E_a is the apparent activation energy (kJ/mol), T is the thermodynamic temperature (K), and R is the molar gas constant (8.314J/(mol·K)).

It can be seen from Fig. 14 that when $1-(1-x)^{1/3}$ is plotted as a function of leaching time t at different temperatures, R^2>0.9, as shown in Table 2. As shown in Fig. 15, the activation energy E_a of the chemical-reaction-controlled step shown

Table 2 Reaction rate constants at different temperatures

Temperature/°C	k/min^{-1}	R^2
40	0.00288	0.989
50	0.00571	0.978
60	0.00944	0.992
70	0.01625	0.999
80	0.02761	0.999

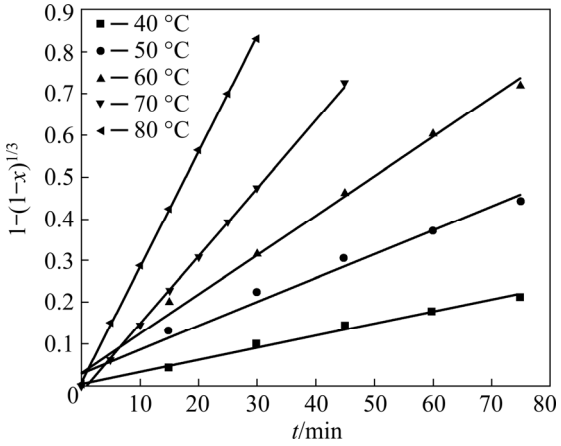

Fig. 14 Plots of $1-(1-x)^{1/3}$ vs leaching time t at different temperatures

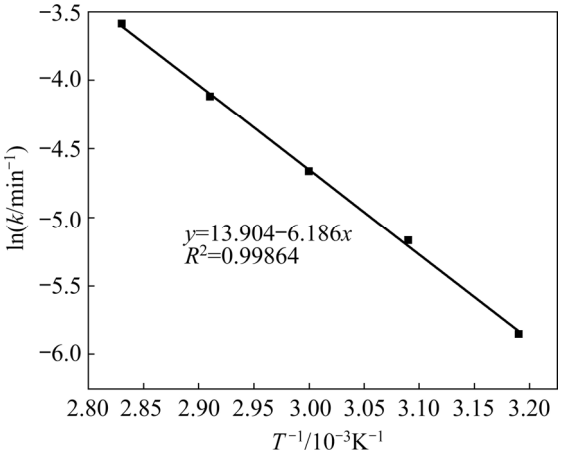

Fig. 15 Arrhenius plot for tungsten leaching in chemical reaction control

in Eq. (8) is 51.43 kJ/mol (>42 kJ/mol), thereby proving that the tungsten leaching process is controlled by chemical reactions [21−23]. In summary, the kinetic equation for tungsten leaching is formulated as Eq. (9):

$$1-(1-x)^{1/3}=\exp(13.90404-6185.7002/T)t \quad (9)$$

3.4 Thermal decomposition of leaching solution

A leaching solution containing hydrogen aqua oxalato tungstate was obtained from scheelite after leaching with sulfuric and oxalic acids. Hydrogen aqua oxalato tungstate can be decomposed into an oxalic acid dihydrate solution and tungstic acid monohydrate solids at temperatures above 80 °C according to Eq. (10) [24]. Tungstic acid monohydrate can release some crystal water due to evaporation, according to Eq. (11):

$$H_2[WO_3(C_2O_4)\cdot H_2O]_{(aq)}+3H_2O= H_2WO_4\cdot H_2O_{(s)}+H_2C_2O_4\cdot 2H_2O_{(aq)} \quad (10)$$

$$H_2WO_4\cdot H_2O_{(s)}=H_2WO_{4(s)}+H_2O \quad (11)$$

The leaching solution was heated at 85 °C for 3 h, and oxalic and tungstic acids were obtained after filtration. The XRD pattern and SEM image of the leaching residue are shown in Fig. 16. The leaching residue had diffraction peaks of tungstic acid monohydrate and tungstic acid, and it mainly contained irregularly shaped lamellae with particle sizes of 0.1−0.5 μm.

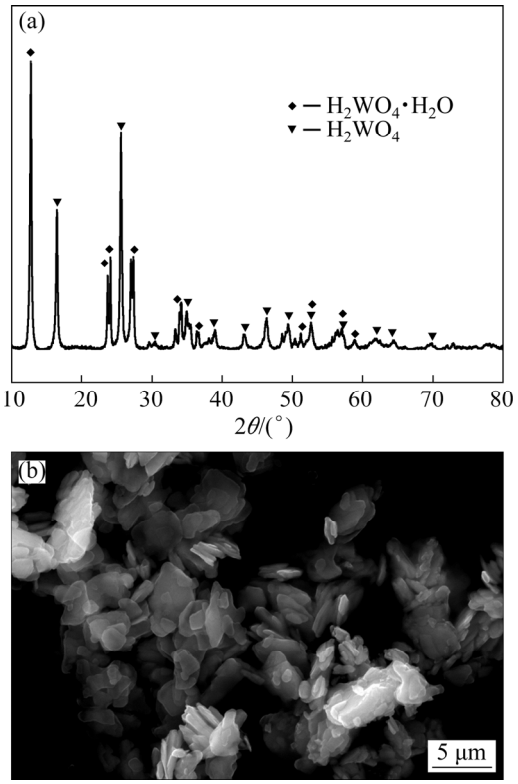

Fig. 16 XRD pattern (a) and SEM image (b) of leaching residue

The tungstic acid was calcined at 700 °C for 2 h to obtain tungsten trioxide, as shown by Eq. (12) [25]:

$$H_2WO_{4(s)}=WO_{3(s)}+H_2O, \quad \Delta_r G^{\Theta}_{700°C}=-14.136 \text{ kJ/mol} \quad (12)$$

Figure 17(a) shows that all major diffraction peaks of the calcined product could be assigned to tungsten trioxide, and no other impurity peaks were detected. This suggests that tungstic acid was completely decomposed into high-purity tungsten trioxide. Figure 17(b) shows the SEM image of the calcined product, where the tungsten trioxide was observed as square plates with particle sizes of 0.5−2 μm.

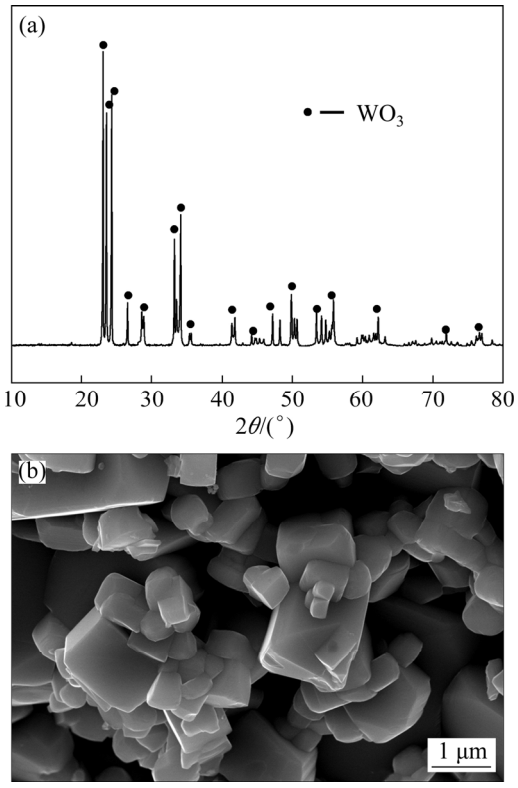

Fig. 17 XRD pattern (a) and SEM image (b) of calcined product

3.5 Flow sheet establishment

A novel technological process of scheelite leaching with sulfuric and oxalic acids was established based on the experiments conducted in this study, as summarized in Fig. 18. Herein, approximately 99.2% of tungsten was leached under the following leaching conditions: stirring

speed, 300 r/min; sulfuric acid concentration, 1.5 mol/L; oxalic acid concentration, 1 mol/L; temperature, 70 °C; liquid/solid ratio, 25:1 mL/g; $n(H_2C_2O_4)/n(H_2SO_4)$ ratio, 1:1; leaching time, 2 h. Calcium was left in the leaching residue in the form of calcium sulfate dihydrate, which could be used to prepare cement to increase its economic value and add further value to the process while minimizing waste products. Tungsten also remained in the leaching solution in the form of hydrogen aqua oxalato tungstate, which could be decomposed into oxalic acid dihydrate solution and tungstic acid solids after treatment at 85 °C for 3 h. Tungstic acid was calcined at 700 °C for 2 h and decomposed into tungsten trioxide for tungsten production. Finally, oxalic acid dihydrate could be recycled to decompose the scheelite concentrate.

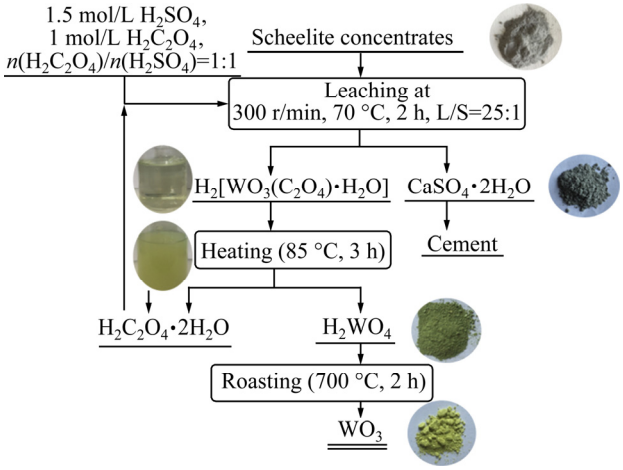

Fig. 18 Flow sheet for leaching tungsten from scheelite concentrates

4 Conclusions

(1) Tungsten could be leached in the form of hydrogen aqua oxalato tungstate from scheelite with sulfuric and oxalic acids. Approximately 99.2% of tungsten was leached under the following leaching conditions: temperature of 70 °C; 1.5 mol/L sulfuric acid; 1 mol/L oxalic acid; liquid/solid ratio of 25:1 (mL/g); $n(H_2C_2O_4)/n(H_2SO_4)$ ratio of 1:1; stirring speed of 300 r/min; leaching time of 2 h.

(2) The leaching kinetics revealed that the leaching of tungsten followed the shrinking core model and was controlled by the chemical reaction step, with an apparent activation energy of 51.43 kJ/mol.

(3) A leaching solution containing hydrogen aqua oxalato tungstate was obtained from scheelite after leaching with sulfuric and oxalic acids. This solution was decomposed to tungstic acid at 85 °C for 3 h. In addition, tungsten trioxide was produced by calcining tungstic acid at 700 °C for 2 h.

Acknowledgments

The authors are grateful for the financial supports from the National Natural Science Foundation of China (Nos. 51564019, 51674125), and the Science and Technology Project of Jiangxi Provincial Education Department, China (No. GJJ181501).

References

[1] YANG Yue, XIE Bo-yi, WANG Rui-xiang, XU Sheng-ming, WANG Jian-long, XU Zhen-he. Extraction and separation of tungsten from acidic high-phosphorus solution [J]. Hydrometallurgy, 2016, 164: 97−102.

[2] WANG Kai-fei, ZHANG Guo-hua. Synthesis of high-purity ultrafine tungsten and tungsten carbide powders [J]. Transactions of Nonferrous Metals Society of China, 2020, 30: 1697−1706.

[3] LI Xiao-bing, SHENG Lei-ting, ZHOU Qiu-sheng, PENG Zhi-lou, LIU Gui-hua, QI Tian-gui. Scheelite conversion in sulfuric acid together with tungsten extraction by ammonium carbonate solution [J]. Hydrometallurgy, 2017, 171: 106−115.

[4] MARTIN J P. Kinetics of soda ash leaching of low grade scheelite concentrates [J]. Hydrometallurgy, 1996, 42: 221−236.

[5] CHEN Xing-yu, CHEN Qiang, GUO Fu-liang, LIAO Yu-long, ZHAO Zhong-wei. Extraction behaviors of rare-earths in the mixed sulfur−phosphorus acid leaching solutions of scheelite [J]. Hydrometallurgy, 2018, 175: 326−332.

[6] CHEN Min, LI Zhao, LI Xue-wen, QU Jun, ZHANG Qi-wu. Mechanochemically extracting tungsten through caustic processing of scheelite by controlling calcium dissolution [J]. International Journal of Refractory Metals and Hard Metals, 2016, 58: 211−215.

[7] WANG Lin-sheng, HUANG Xiao-jing, DENG Deng-fei, LI Hong-chao, CHEN Yao-ming. Synthesis of scheelite from sodium tungsten solution by calcium hydroxide addition [J]. Hydrometallurgy, 2015, 154: 17−19.

[8] ZHAO Zhong-wei, HU Fang, HU Yu-jie, WANG Shi-bo, SUN Pei-mei, HUO Guo-sheng, LI Hong-gui. Adsorption behaviour of WO_4^{2-} onto 201 × 7 resin in highly concentrated tungstate solution [J]. International Journal of Refractory Metals and Hard Metals, 2010, 28: 63−67.

[9] LI Ting-ting, SHEN Yan-bei, ZHAO Si-kai, YIN Yao-yu, LU Rui, GAO Shu-ling, HAN Cong, WEI De-zhou. Leaching kinetics of scheelite concentrate with sodium hydroxide in the presence of phosphate [J]. Transactions of

Nonferrous Metals Society of China, 2019, 29: 634−640.
[10] ZHANG Wen-jun, YANG Jing-hong, ZHAO Zhong-wei, WANG Wen-qiang, LI Jiang-tao. Coordination leaching of tungsten from scheelite concentrate with phosphorus in nitric acid [J]. Journal of Central South University, 2016, 23: 1312−1317.
[11] ZHANG Wen-juan, LI Jiang-tao, ZHAO Zhong-wei. Leaching kinetics of scheelite with nitric acid and phosphoric acid [J]. International Journal of Refractory Metals and Hard Metals, 2015, 52: 78−84.
[12] LI Wei-qiang. Investigation on low-concentrate and low-addition HCl digestion of scheelite concentrate [J]. Rare Metals and Cemented Carbides, 1998, 132: 5−8.
[13] LI Jiang-tao, ZHAO Zhong-wei. Kinetics of scheelite concentrate digestion with sulfuric acid in the presence of phosphoric acid [J]. Hydrometallurgy, 2016, 163: 55−60.
[14] KALPAKLI A O, ILHAN S, KAHRUMAN C, YUSUFOGLU I. Dissolution behavior of calcium tungstate in oxalic acid solutions [J]. Hydrometallurgy, 2012, 121−124: 7−15.
[15] XU Xiang-ming, ZHOU Ke-chao, LI Xiao-bin, ZHOU Qiu-sheng, QI Tian-gui, LIU Gui-hua, PENG Zhi-lou. Leaching of synthetic Ca_3WO_6 with ammoniacal ammonium carbonate solution under atmospheric pressure: A fundamental study [J]. Hydrometallurgy, 2019, 184: 55−66.
[16] TAVAKOLI M R, DREISINGER D B. The kinetics of oxidative leaching of vanadium Trioxide [J]. Hydrometallurgy, 2014, 147: 83−89.
[17] TIAN Lei, LIU Yan, ZHANG Ting-an, LV Guo-zhi, ZHOU Shuang, ZHANG Guo-quan. Kinetics of indium dissolution from marmatite with high indium content in pressure acid leaching [J]. Rare Metals, 2017, 36(1): 69−76.
[18] WANG H H, LI G Q, ZHAO D, MA J H, YANG J. Dephosphorization of high phosphorus oolitic hematite by acid leaching and the leaching kinetics [J]. Hydrometallurgy, 2017, 171: 61−68.
[19] MESHRAM M, PANDEY B D, MANKHAND T R. Recovery of valuable metals from cathodic active material of spent lithium ion batteries: Leaching and kinetics aspects [J]. Waste Management, 2015, 45: 306−313.
[20] GONG Dan-dan, ZHOU Kang-gen, PENG Chang-hong, HE De-wen, CHEN Wei. Resin-enhanced acid leaching of tungsten from scheelite [J]. Hydrometallurgy, 2018, 182: 75−81.
[21] CHOI I H, MOON G, LEE J Y, JYOTHI R K. Extraction of tungsten and vanadium from spent selective catalytic reduction catalyst for stationary application by pressure leaching process [J]. Journal of Cleaner Production, 2018, 197: 163−169.
[22] SHENG Lei-ting, LI Xiao-bing, ZHOU Qiu-sheng, PENG Zhi-lou, LIU Gui-hua, QI Tian-gui, TASKINEN P. Sustainable and efficient leaching of tungsten in ammoniacal ammonium carbonate solution from the sulfuric acid converted product of scheelite [J]. Journal of Cleaner Production, 2018, 197: 690−698.
[23] SHEN Lei-ting, LI Xiao-bing, ZHOU Qiu-sheng, PENG Zhi-hong, LIU Gui-hua, QI Tian-gui, TASKINEN P. Kinetics of scheelite conversion in sulfuric acid [J]. JOM, 2018, 70: 2499−2504.
[24] ILHAN S, KALPAKLI A O, KAHRUMAN C, YUSUFOGLU I. The investigation of dissolution behavior of gangue materials during the dissolution of scheelite concentrate in oxalic acid solution [J]. Hydrometallurgy, 2013, 136: 15−26.
[25] CAO Jing, LUO Bang-de, LIN Hai-li, XU Ben-yan, CHEN Shi-fu. Thermodecomposition synthesis of WO_3/H_2WO_4 heterostructures with enhanced visible light photocatalytic properties [J]. Applied Catalysis B: Environmental, 2012, 111−112: 288−296.

硫酸−草酸络合浸出白钨矿及含钨相的转化行为

刘庆生[1]，涂 弢[1,2]，郭 浩[3]，程华金[1]，王学重[1]

1. 江西理工大学 材料冶金化学学部，赣州 341000；
2. 赣南科技学院 机电工程系，赣州 341000；
3. 江苏大学 材料科学与工程学院，镇江 212013

摘 要：以草酸为络合剂，利用硫酸从白钨矿中提取钨。在浸出过程中，钨以高水溶性 $H_2[WO_3(C_2O_4)\cdot H_2O]$ 的形式完全浸出，而钙则以 $CaSO_4\cdot 2H_2O$ 的形式残留在渣中。在温度 70 °C、1.5 mol/L 硫酸、1 mol/L 草酸、液固比 25:1 (mL/g)、草酸/硫酸摩尔比 1:1、搅拌速度 300 r/min、浸出时间 2 h 的条件下，钨的浸出率为 99.2%。$H_2[WO_3(C_2O_4)\cdot H_2O]$经热分解转化为 H_2WO_4，H_2WO_4 在 700 °C 下焙烧 2 h，可直接分解成 WO_3。冶金动力学研究表明，白钨矿浸出过程由表面化学反应控制，其表观活化能为 51.43 kJ/mol。

关键词：白钨矿；动力学；化学反应；草酸；硫酸

(Edited by Wei-ping CHEN)